

H¹-STABILITY OF THE L²-PROJECTION ONTO FINITE ELEMENT SPACES ON ADAPTIVELY REFINED QUADRILATERAL MESHES

MAZEN ALI

Centrale Nantes, LMJL UMR CNRS 6629, France

STEFAN A. FUNKEN AND ANJA SCHMIDT

Ulm University, Institute for Numerical Mathematics, Germany

ABSTRACT. The L^2 -orthogonal projection $\Pi_h : L^2(\Omega) \rightarrow \mathbb{V}_h$ onto a finite element (FE) space \mathbb{V}_h is called H^1 -stable iff $\|\nabla \Pi_h u\|_{L^2(\Omega)} \leq C \|u\|_{H^1(\Omega)}$, for any $u \in H^1(\Omega)$ with a positive constant $C \neq C(h)$ independent of the mesh size $h > 0$. In this work, we discuss local criteria for the H^1 -stability of adaptively refined meshes. We show that adaptive refinement strategies for quadrilateral meshes in 2D (Q-RG and Q-RB), introduced originally in Bank et al. 1982 and Kobbelt 1996, are H^1 -stable for FE spaces of polynomial degree $p = 2, \dots, 9$.

1. INTRODUCTION

Let $\Omega \subset \mathbb{R}^d$ be a bounded domain and $\mathbb{V}_h \subset H^1(\Omega)$ a finite element (FE) space on Ω . The H^1 -stability of the L^2 -orthogonal projection $\Pi_h : L^2(\Omega) \rightarrow \mathbb{V}_h$ plays a key role in the analysis of FE methods. To mention a few examples: in [23], the authors show that H^1 -stability is equivalent to the inf-sup stability and quasi-optimality of Galerkin methods for parabolic equations; H^1 -stability is used in the analysis of multi-grid methods (see [26]), boundary element methods (see [19, 21, 22]), and adaptive methods (see [2]). See also [10, 25] for other applications.

For any given finite-dimensional \mathbb{V}_h , we trivially have $\|\nabla \Pi_h u\|_{L^2} \leq C \|u\|_{H^1}$ due to the equivalence of norms on finite-dimensional spaces. However, in general the constant $C = C(h)$ will depend on the dimension of \mathbb{V}_h or, equivalently, mesh size $h > 0$. The issue of H^1 -stability is thus showing the constant $C \neq C(h)$ does not depend on the dimension of \mathbb{V}_h .

It can be shown that for H^1 -stability it is sufficient to show stability in a weighted L^2 -norm

$$(1.1) \quad \sum_{T \in \mathcal{T}} h_T^{-2} \|\Pi_h u\|_{L^2(T)}^2 \lesssim \sum_{T \in \mathcal{T}} h_T^{-2} \|u\|_{L^2(T)}^2,$$

see Section 2.2 for more details. The above estimate is straight-forward if \mathcal{T} is assumed to be quasi-uniform, i.e., $(\max_T h_T)/(\min_T h_T) \sim 1$. However, quasi-uniformity does not hold in general for adaptively refined meshes.

1.1. Previous Work. Before we state the main contribution of this work, we briefly review the key difficulties of showing H^1 -stability and previous results on this subject.

1.1.1. Global Growth Condition. In [12] (CT) the authors suggest criteria based on the localization properties of the FE space \mathbb{V}_h and the rate at which the element size h_T may vary. Namely, for any $u \in L^2(\Omega)$, we can write¹ $u = \sum_{T \in \mathcal{T}} u_T$, with each u_T supported only on T . The localization property of Π_h from CT can be described by a function $\gamma(T, \bar{T}) \geq 0$, decreasing with the distance between T and \bar{T} , such that

$$\|\Pi_h u_T\|_{L^2(\bar{T})} \leq \gamma(T, \bar{T}) \|u_T\|_{L^2(\Omega)}.$$

E-mail addresses: mazen.ali@ec-nantes.fr, {stefan.funken,anja.schmidt}@uni-ulm.de.

Date: September 1, 2020.

2010 Mathematics Subject Classification. 65M50.

Key words and phrases. H^1 -Stability, L^2 -Projection, Finite Elements, Quadrilateral Mesh, Adaptive Refinement.

¹Assuming the meshing of Ω is exact.

Then, for any $T \in \mathcal{T}$ we can estimate

$$h_T^{-1} \|\Pi_h u\|_{L^2(T)} \leq h_T^{-1} \sum_{\bar{T} \in \mathcal{T}} \gamma(T, \bar{T}) \|u_{\bar{T}}\|_{L^2(T)} = \sum_{\bar{T} \in \mathcal{T}} \gamma(T, \bar{T}) \frac{h_{\bar{T}}}{h_T} h_{\bar{T}}^{-1} \|u_{\bar{T}}\|_{L^2(T)}.$$

Summing over $T \in \mathcal{T}$, we can thus show eq. (1.1) if we can bound

$$(1.2) \quad \sum_{\bar{T} \in \mathcal{T}} \gamma(T, \bar{T}) \frac{h_{\bar{T}}}{h_T} \lesssim 1,$$

independently of $T \in \mathcal{T}$.

The issue of H^1 -stability hinges on the interplay between the localization property of Π_h and the variation in size $h_T/h_{\bar{T}}$. For common refinement strategies, e.g., newest vertex bisection (NVB) or red green blue (RGB) refinement, the ratio $h_T/h_{\bar{T}}$ may grow exponentially, in the worst case; while $\|\Pi_h u_T\|_{L^2(\bar{T})}$ will decay exponentially. Whether eq. (1.2) is satisfied then depends on the factors in the exponents of the growth/decay of both quantities.

E.g., eq. (1.2) is trivially satisfied for the non-conforming case, see Theorem 2.9. It is also satisfied for any projection for which the support of $\Pi_h u_T$ is finite, as is the case for quasi-interpolation (Clément-type) operators (see also Assumption 2.4). Finally, we note that H^1 -stability of the L^2 -projection is closely related to the question of the decay of the entries of the inverse of the mass-matrix away from the diagonal, see [13].

1.1.2. Element-Wise Criteria. The CT criterion (1.2) illustrates the main issues of showing H^1 -stability and all criteria proposed thereafter are essentially based on the same idea. However, eq. (1.2) is not easy to verify for common adaptive refinement strategies.

In [6] (BPS) the authors propose a criteria that can be verified locally on an element $T \in \mathcal{T}$. In [7] (CC) this was generalized to more flexible criteria that can also be locally verified, and where BPS and CT can be seen as specific instances of the CC criteria.

In [4] (BY) the authors suggest criteria that can be verified by computing (small) eigenvalue problems. Though BY uses a proof technique different from CC, it can be in fact seen as a particular instance of CC, with the difference being that BY is easier to verify, see also Remark 3.5 for more details.

In [16] all of the above criteria are summarized into a single framework that is both most flexible and easiest to verify. Finally, in [8, 15, 17] the above criteria were applied to show H^1 -stability for adaptively refined triangular meshes in 2D.

1.2. This Work. We condense the aforementioned criteria to a general framework that, in principle, can be applied in any dimension to meshes \mathcal{T} consisting of arbitrary elements, with or without hanging nodes, and of arbitrary polynomial order $p \in \mathbb{N}_0$. We briefly show that for the non-conforming case $\mathbb{V}_h \not\subset H^1(\Omega)$ stability is straight-forward and requires no additional assumptions. We specify criteria for the H^1 -stability of regular and 1-irregular meshes in 2D, consisting of triangles, general quadrilaterals, mixtures thereof, with 0, 1 or 2 hanging nodes per element, for various polynomial degrees $p \in \mathbb{N}$. Our **main results** are Theorems 4.6 and 4.9 where we show that the adaptive refinement strategies for quadrilaterals Q-RG and Q-RB from [3, 14, 18] are H^1 -stable for polynomial degrees $p = 2, \dots, 9$.

Outline. In Section 2, we discuss a general framework for verifying H^1 -stability. We show in Section 2.3 that the non-conforming case does not require additional assumptions. In Section 3, we specify computable criteria and comment in more detail on some practical aspects of verifying H^1 -stability. Our main results are contained in Section 4, where we state criteria for H^1 -stability of general triangular/quadrilateral meshes in 2D, recall adaptive refinement strategies from [14] and prove H^1 -stability for Q-RG and Q-RB. In Appendix A, we list tables of eigenvalues required for verifying H^1 -stability criteria. The corresponding code can be found in [1].

Notation. We use $A \lesssim B$ for quantities $A, B \in \mathbb{R}$ to indicate $A \leq CB$ for some constant $C \geq 0$ independent of A or B . Similarly $A \gtrsim B$ and $A \sim B$ if both \lesssim and \gtrsim hold. We use the following shorthand notation

$$\begin{aligned} \|u\|_0 &:= \|u\|_{L^2(\Omega)}, & \|u\|_1 &:= \|u\|_{H^1(\Omega)}, & \|u\|_{0,T} &:= \|u\|_{L^2(T)}, \\ \|h^{-1}u\|_0^2 &:= \sum_{T \in \mathcal{T}} h_T^{-2} \|u\|_{0,T}^2, & \langle u, v \rangle_0 &:= \langle u, v \rangle_{L^2(\Omega)}, & \langle u, v \rangle_T &:= \langle u, v \rangle_{L^2(T)}. \end{aligned}$$

Finally, we use $|T|$ to denote the Lebesgue \mathbb{R}^d -measure of T and $\#\mathcal{T}$ to denote the standard counting measure of \mathcal{T} .

2. A GENERAL FRAMEWORK FOR H^1 -STABILITY

There are several sufficient criteria for the H^1 -stability of the L^2 -projection available in the literature, see [4, 6, 7, 12]. These criteria were successfully applied to triangular meshes in 2D, see [8, 15, 17]. All of these criteria have a common underlying idea as explained in Section 1.1.

In this section, we condense all of the aforementioned criteria to a single unifying framework which can be applied to either triangular or quadrilateral meshes, mixtures thereof, or more general meshes.

2.1. The Mesh and Finite Element Space. Let $\Omega \subset \mathbb{R}^d$ be a bounded domain and $\mathcal{T} := \{T_1, \dots, T_N\}$, $N \in \mathbb{N}$ a finite set of closed convex polytopes $T_i \subset \Omega$ which we refer to as *elements*. We make the following assumptions on \mathcal{T} .

Definition 2.1 (Admissible Mesh). *We call a mesh \mathcal{T} admissible if*

- (i) *it is exact, i.e., $\bar{\Omega} = \bigcup_{T \in \mathcal{T}} T$,*
- (ii) *the elements $T \in \mathcal{T}$ are non-empty $T \neq \emptyset$ and non-overlapping, i.e.,*

$$\mathring{T}_i \cap \mathring{T}_j = \emptyset, \quad T_i \neq T_j,$$

where \mathring{T} denotes the interior of T ;

- (iii) *the mesh \mathcal{T} is shape-regular. That is, for any $T \in \mathcal{T}$, let ρ_T denote the diameter of the largest ball still contained in T and let h_T denote the diameter of T*

$$h_T := \text{diam}(T) := \sup_{x, y \in T} \|x - y\|_2.$$

Then, we assume $\rho_T \sim h_T$, with a constant independent of T . This also implies $h_T^d \sim |T|$, where we use $|T|$ to denote the Lebesgue \mathbb{R}^d -measure of T .

Let $H^1(\Omega)$ denote the Sobolev space of square-integrable functions on Ω with one weak square-integrable derivative. We define the sets of *complete* and *incomplete* polynomials over an element T , respectively

$$(2.1) \quad \begin{aligned} \mathcal{P}_p(T) &:= \text{span} \left\{ x \mapsto x_1^{p_1} \cdots x_d^{p_d} : p_i \in \mathbb{N}_0, \sum_{i=1}^d p_i \leq p, x = (x_1, \dots, x_d)^\top \in T \right\}, \\ \mathcal{Q}_p(T) &:= \text{span} \left\{ x \mapsto x_1^{p_1} \cdots x_d^{p_d} : p_i \in \mathbb{N}_0, p_i \leq p, x = (x_1, \dots, x_d)^\top \in T \right\}. \end{aligned}$$

Definition 2.2 (Conforming FE Space). *Let \mathcal{T} be an admissible mesh and fix a polynomial degree $p \in \mathbb{N}$. A conforming piece-wise polynomial FE space of polynomial degree p is any space $\mathbb{V}_h = \mathbb{V}_h(\mathcal{T}, p)$ such that*

$$\mathbb{V}_h = \mathbb{V}_h(\mathcal{T}, p) = \{v_h \in H^1(\Omega) : (v_h)|_T \in \mathbb{P}_p(T), T \in \mathcal{T}\},$$

where $\mathbb{P}_p(T) \in \{\mathcal{P}_p(T), \mathcal{Q}_p(T)\}$, i.e., $(v_h)|_T$ is either² a complete or incomplete polynomial of degree p . We denote the associated L^2 -orthogonal projection by $\Pi_h : L^2(\Omega) \rightarrow \mathbb{V}_h$. Here the subscript h is used to indicate FE spaces and functions.

We use $\mathcal{V}(\mathcal{T})$ to denote the set of vertices of all elements T , i.e., the set of extreme points. We associate to each FE space \mathbb{V}_h a finite set of (Lagrange) nodes $\mathcal{N} := \mathcal{N}(\mathcal{T}) \subset \Omega$ and a set of basis functions

$$\Phi_{\mathcal{N}} := \{\varphi_a : a \in \mathcal{N}(\mathcal{T})\},$$

such that $\mathbb{V}_h = \text{span } \Phi_{\mathcal{N}}$. We set $\mathcal{V}(T) := \mathcal{V}(\mathcal{T}) \cap T$. Finally, for $S_a^T := \{x \in T : \varphi_a(x) \neq 0\}$, we define

$$(2.2) \quad \mathcal{N}(T) := \{a \in \mathcal{N} : |S_a^T| > 0\}.$$

Remark 2.3.

²Note that this permits some ambiguity as there can be (finitely many) spaces $\mathbb{V}_h(\mathcal{T}, p)$ that are conforming piece-wise polynomial FE spaces of degree p . The same is true since we, strictly speaking, allow for $\mathbb{V}_h \subset H^s(\Omega)$, $s > 1$. However, this does not impact the theory presented here, as long as we fix the choice of \mathbb{V}_h . In Section 4, this choice will be made clear.

- (i) The conformity $\mathbb{V}_h \subset H^1(\Omega)$ is necessary to ensure $\|\nabla \Pi_h u\|_0$ is well-defined. Since functions in \mathbb{V}_h are polynomial except on a set of Lebesgue measure zero, $v_h \in H^1(\Omega)$ holds if and only if $v_h \in C(\Omega)$, or, equivalently, if v_h is continuous along the interior boundary $\partial T \setminus \partial\Omega$ of $T \in \mathcal{T}$.
- (ii) For ease of notation we do not consider boundary conditions on $\partial\Omega$, but all of the subsequent results apply to this case as well.
- (iii) An important consequence of shape-regularity is that for any $T \in \mathcal{T}$ and any $v_h \in \mathbb{V}_h$,

$$\|\nabla v_h\|_{0,T} \lesssim h_T^{-1} \|v_h\|_{0,T}.$$

2.2. General Criteria for H^1 -Stability. The stability of Π_h in the H^1 -norm can be reduced to the stability of Π_h in a weighted L^2 -norm through the use of a stable interpolation operator.

Assumption 2.4 (Stable Quasi-Interpolation Operator). *We assume the existence of a (possibly non-linear) mapping $Q_h : H^1(\Omega) \rightarrow \mathbb{V}_h$ that satisfies*

$$(2.3) \quad \|\nabla Q_h u\|_0 + \|h^{-1}(u - Q_h u)\|_0 \lesssim \|u\|_1, \quad \forall u \in H^1(\Omega),$$

where $h^{-1} : \Omega \rightarrow \mathbb{R}$ is the piece-wise constant function $h^{-1} := \sum_{T \in \mathcal{T}} h_T^{-1} \mathbb{1}_T$, with the indicator functions $\mathbb{1}_T$.

An example of such a mapping Q_h is the Clément operator [11] and variants thereof, see also [20]. Specifically for this work we can use the flexible construction from [9], which applies to both triangular and quadrilateral meshes, with or without hanging nodes.

Lemma 2.5 (Stability in a Weighted L^2 -Norm). *Let \mathcal{T} be an admissible mesh and let Assumption 2.4 hold. If $\Pi_h : L^2(\Omega) \rightarrow \mathbb{V}_h$ satisfies*

$$(2.4) \quad \|h^{-1} \Pi_h u\|_0 \lesssim \|h^{-1} u\|_0, \quad \forall u \in H^1(\Omega),$$

then $\|\nabla \Pi_h u\|_0 \lesssim \|u\|_1$ holds.

Proof. This is a simple consequence of the triangle inequality, property (2.3) and shape-regularity

$$\|\nabla \Pi_h u\|_0 = \|\nabla \Pi_h(u - Q_h u) + \nabla Q_h u\|_0 \lesssim \|h^{-1}(u - Q_h u)\|_0 + \|\nabla Q_h u\|_0 \lesssim \|u\|_1. \quad \square$$

We are thus left with showing (2.4). To this end, we will use the following general criteria.

Assumption 2.6 (H^1 -stability Criteria). *We assume there exist (possibly non-linear) mappings $H_+, H_- : \mathbb{V}_h \rightarrow \mathbb{V}_h$ that satisfy*

(C1) *the mapping H_+ is invertible and the inverse H_+^{-1} satisfies*

$$\|h^{-1} v_h\|_0 \lesssim \|H_+^{-1} v_h\|_0, \quad \forall v_h \in \mathbb{V}_h,$$

(C2) *the mapping H_- satisfies*

$$\|h H_- v_h\|_0 \lesssim \|v_h\|_0, \quad \forall v_h \in \mathbb{V}_h,$$

(C3) *the mappings H_+ and H_- jointly satisfy*

$$\|v_h\|_0^2 \lesssim \langle H_+ v_h, H_- v_h \rangle_0, \quad \forall v_h \in \mathbb{V}_h.$$

Different versions of the following theorem can be found in [6, 7, 16] for specific choices of H_+, H_- . We include the simple proof here for completeness.

Theorem 2.7 (H^1 -stability [6, 7, 16]). *Let \mathcal{T} be an admissible mesh and let Assumption 2.4 and Assumption 2.6 hold. Then, the L^2 -orthogonal projection $\Pi_h : L^2(\Omega) \rightarrow \mathbb{V}_h$ is H^1 -stable in the sense*

$$\|\nabla \Pi_h u\|_0 \lesssim \|u\|_1, \quad \forall u \in H^1(\Omega).$$

Proof. By (C2), (C3) and L^2 -orthogonality of Π_h

$$\begin{aligned} \|H_+^{-1} \Pi_h u\|_0^2 &\lesssim \langle \Pi_h u, H_- H_+ \Pi_h u \rangle_0 = \langle h^{-1} u, h H_- H_+ \Pi_h u \rangle_0 \leq \|h^{-1} u\|_0 \|h H_- H_+^{-1} \Pi_h u\|_0 \\ &\lesssim \|h^{-1} u\|_0 \|H_+^{-1} \Pi_h u\|_0, \end{aligned}$$

and thus $\|H_+^{-1} \Pi_h u\|_0 \lesssim \|h^{-1} u\|_0$. From (C1) we get $\|h^{-1} \Pi_h u\|_0 \lesssim \|H_+^{-1} \Pi_h u\|_0$. Together with Lemma 2.5, this completes the proof. \square

Remark 2.8 (Alternative Criteria). *There is an alternative to criteria (C1) – (C3), which requires fewer assumptions. Namely, suppose there exists a linear operator $H_- : \mathbb{V}_h \rightarrow \mathbb{V}_h$ that satisfies*

(1) for any $v_h \in \mathbb{V}_h$

$$\|h^{-1}v_h\|_0 \lesssim \|H_-v_h\|_0,$$

(2) and for any $v_h \in \mathbb{V}_h$

$$\|h(H_-)^*H_-v_h\|_0 \lesssim \|h^{-1}v_h\|_0,$$

where $(H_-)^*$ denotes the Hilbert adjoint of H_- .

Then, analogously to Theorem 2.7, we can show

$$\begin{aligned} \|h^{-1}\Pi_h u\|_0^2 &\lesssim \|H_- \Pi_h u\|_0^2 = \langle (H_-)^* H_- \Pi_h u, \Pi_h u \rangle_0 = \langle (H_-)^* H_- \Pi_h u, u \rangle \\ &= \langle h(H_-)^* H_- \Pi_h u, h^{-1}u \rangle \leq \|h(H_-)^* H_- \Pi_h u\|_0 \|h^{-1}u\|_0 \lesssim \|h^{-1}\Pi_h u\|_0 \|h^{-1}u\|_0. \end{aligned}$$

The issue with this criteria is that, having specified H_- , it requires computing the adjoint $(H_-)^*$. In particular, even if H_- has a simple “local” definition³, H_-^* will still be non-local in general. In contrast, criteria (C1) – (C3) allow for the flexibility of choosing a local map H_+ .

2.3. The Non-Conforming Case. Alternatively, we could consider H^1 -stability of non-conforming FE spaces in the broken Sobolev norm. The gradient $\nabla : H^1(\Omega) \rightarrow L^2(\Omega)$ is replaced by the piece-wise gradient $(\nabla_{\mathcal{T}}u)|_T := \nabla(u|_T)$ for every $T \in \mathcal{T}$. The broken Sobolev space is defined as

$$H^1(\mathcal{T}) := \{u \in L^2(\Omega) : u|_T \in H^1(T), T \in \mathcal{T}\},$$

and the corresponding FE space as

$$\mathbb{V}_h^B := \{(v_h)|_T \in \mathbb{P}_p(T), T \in \mathcal{T}\}.$$

Then, the corresponding L^2 -projection $\Pi_h^B : L^2(\Omega) \rightarrow \mathbb{V}_h^B$ is said to be H^1 -stable if

$$\|\nabla_{\mathcal{T}}\Pi_h^B u\|_0 \lesssim \|u\|_{H^1(\mathcal{T})}, \quad \forall u \in H^1(\mathcal{T}).$$

However, in this case H^1 -stability is trivially satisfied for any admissible mesh that satisfies Assumption 2.4.

Theorem 2.9 (H^1 -stability Discontinuous FE). *Let \mathcal{T} be an admissible mesh satisfying Assumption 2.4 (with the definition of norms adjusted accordingly). Then, the L^2 -projection $\Pi_h^B : L^2(\Omega) \rightarrow \mathbb{V}_h^B$ is H^1 -stable.*

Proof. Let $u_T \in L^2(\Omega)$ be an arbitrary L^2 -function supported on $T \in \mathcal{T}$. Let w_T be the $L^2(T)$ -orthogonal projection of u_T onto $\mathbb{P}_p(T)$, which we extend with zero on $\Omega \setminus T$. Then, clearly $w_T \in \mathbb{V}_h^B$ and, on one hand, $\|u_T - w_T\|_0 \geq \|u_T - \Pi_h^B u_T\|_0$. On the other hand,

$$\|u_T - w_T\|_0^2 = \sum_{\bar{T} \in \mathcal{T}} \|u_T - w_T\|_{0,\bar{T}}^2 \leq \sum_{\bar{T} \in \mathcal{T}} \|u_T - \Pi_h^B u_T\|_{0,\bar{T}}^2 = \|u_T - \Pi_h^B u_T\|_0^2,$$

and thus $\|u_T - w_T\|_0 = \|u_T - \Pi_h^B u_T\|_0$. Since $\mathbb{V}_h^B \subset L^2(\Omega)$ is compact, the orthogonal projection is unique and thus $w_T = \Pi_h^B u_T$.

In particular, this implies

$$\|\Pi_h^B u_T\|_{0,\bar{T}} = 0, \quad \text{for any } \bar{T} \neq T.$$

Since Π_h is an orthogonal projection, we also have $\|\Pi_h^B u_T\|_0 \leq \|u_T\|_0$.

For any $u \in H^1(\mathcal{T})$, we can write $u = \sum_{T \in \mathcal{T}} u_T$ with $u_T := u|_T$ and observe $\Pi_h^B u = \sum_{T \in \mathcal{T}} \Pi_h^B u_T$. Thus $\|\Pi_h^B u\|_{0,T} = \|\Pi_h^B u_T\|_0$ and

$$\|h^{-1}\Pi_h^B u\|_0^2 = \sum_{T \in \mathcal{T}} h_T^{-2} \|\Pi_h^B u_T\|_0^2 = \sum_{T \in \mathcal{T}} h_T^{-2} \|\Pi_h^B u_T\|_0^2 \leq \sum_{T \in \mathcal{T}} h_T^{-2} \|u_T\|_0^2 = \|h^{-1}u\|_0^2.$$

Together with Lemma 2.5 (adjusted for the broken Sobolev norm), this shows the H^1 -stability of Π_h^B . \square

³In the sense that will become clear in Section 3.

3. COMPUTABLE CRITERIA FOR H^1 -STABILITY

In this section, we discuss a particular choice for the mappings H_+ and H_- . First, we briefly motivate how a “practical” choice for H_+ , H_- would look like.

Let $\{\mathcal{T}_n\}_{n=0}^\infty$ be a sequence of finer meshes with $\#\mathcal{T}_n \rightarrow \infty$ and let Π_{h_n} denote the corresponding L^2 -projections. For this particular sequence, H^1 -stability means we have

$$\|\nabla \Pi_{h_n} u\|_0 \leq C \|u\|_1, \quad \forall u \in H^1(\Omega),$$

for some $C \neq C(n)$ independent of $n \in \mathbb{N}$. The sequence $\{\mathcal{T}_n\}_{n=0}^\infty$ may depend, among other things, on the initial discretization, the problem to be solved (such as a partial differential equation), the choice of marking strategy (e.g., error estimator), the choice of adaptive refinement strategy and so on.

For this reason disproving H^1 -stability can be particularly difficult: even if $C = C(n) \rightarrow \infty$ for some artificially constructed sequence $\{\mathcal{T}_n\}_{n=0}^\infty$, we can still have a class of problems and a set of marking rules for which $\{\mathcal{T}_n\}_{n=0}^\infty$ will always remain H^1 -stable. Thus, proofs of H^1 -stability as in [8, 15, 17] focus solely on the refinement strategy (e.g., RGB, NVB, RG, etc.). This necessarily results in the (much stronger) *local* conditions, i.e., the conditions of Assumption 2.6 are replaced with

$$(3.1) \quad \|h^{-1}v_h\|_{0,T} \lesssim \|H_+^{-1}v_h\|_{0,T}, \quad \|hH_-v_h\|_{0,T} \lesssim \|v_h\|_{0,T}, \quad \|v_h\|_{0,T}^2 \lesssim \langle H_+v_h, H_-v_h \rangle_{0,T},$$

for any $T \in \mathcal{T}$ and any $v_h \in \mathbb{V}_h$.

3.1. Verifying (C1) – (C2). In [6, 7, 16] the authors consider locally defined weight functions as follows.

Lemma 3.1 (Choice of H_+ , H_- [6, 7, 16]). *Let $\{h_a^+ : a \in \mathcal{N}\}$ and $\{h_a^- : a \in \mathcal{N}\}$ be sets of positive weights $h_a^+, h_a^- > 0$. We define the mapping $H_+ : \mathbb{V}_h \rightarrow \mathbb{V}_h$ as*

$$H_+(v_h) = H_+ \left(\sum_{a \in \mathcal{N}} c_a \varphi_a \right) := \sum_{a \in \mathcal{N}} h_a^+ c_a \varphi_a,$$

and analogously $H_- : \mathbb{V}_h \rightarrow \mathbb{V}_h$. If the weights satisfy for any $T \in \mathcal{T}$

$$h_a^+ \sim h_T, \quad h_a^- \sim h_T^{-1}, \quad \forall a \in \mathcal{N}(T),$$

then H_+ and H_- satisfy (C1) – (C2).

Proof. By the definition of the index set $\mathcal{N}(T)$ (see (2.2)), we have for any $T \in \mathcal{T}$ and any $v_h = \sum_{a \in \mathcal{N}} c_a \varphi_a \in \mathbb{V}_h$

$$\|h^{-1}v_h\|_{0,T} = \left\| \sum_{a \in \mathcal{N}(T)} h_T^{-1} c_a \varphi_a \right\|_{0,T} \lesssim \left\| \sum_{a \in \mathcal{N}(T)} h_a^{-1} c_a \varphi_a \right\|_{0,T} = \|H_+^{-1}v_h\|_{0,T},$$

and consequently $\|h^{-1}v_h\|_0 \lesssim \|H_+^{-1}v_h\|_0$. Analogously for (C2). \square

3.2. Verifying (C3). The last condition can be verified by solving a local generalized eigenvalue problem. We namely have

$$\|v_h\|_{0,T}^2 \lesssim \langle H_+v_h, H_-v_h \rangle_{0,T} = \langle v_h, (H_+)^* H_-v_h \rangle_{0,T} = \left\langle v_h, \frac{1}{2}(H_+^* H_- + H_-^* H_+)v_h \right\rangle_{0,T}.$$

This amounts to assembling the local mass-matrix $M(T)$

$$(M(T))_{a,b} := \langle \varphi_a, \varphi_b \rangle_{0,T} \quad a, b \in \mathcal{N}(T),$$

the weighted matrix $A(T)$

$$(A(T))_{a,b} := \frac{1}{2} (h_a^+ h_b^- + h_b^+ h_a^-) (M(T))_{a,b}, \quad a, b \in \mathcal{N}(T),$$

and solving the generalized eigenvalue problem

$$(3.2) \quad A(T)x = \lambda M(T)x, \quad x \in \mathbb{R}^{\#\mathcal{N}(T)}.$$

If the smallest eigenvalue of (3.2) $\lambda_{\min} > 0$ is positive, then (C3) holds for a positive constant $C := \lambda_{\min}^{-1}$. Moreover, if T can be obtained by an affine transformation $B_T : \hat{T} \rightarrow T$ from some reference element \hat{T} , then the minimal eigenvalue in (3.2) does not depend on T . We comment more on this in Remark 4.2 and we address the case of non-linear transformations $B_T : \hat{T} \rightarrow T$ in Section 4.3.

3.3. Weights Based on the Refinement Level. In [7, 15, 16] the authors consider weights based on the refinement level of an element and a distance function. We will use the same type of function for this work.

Definition 3.2 (Generation of an Element). *For a sequence $\{\mathcal{T}_n\}_{n=0}^\infty$, we assume⁴ that any $T \in \mathcal{T}_n$, for any $n \in \mathbb{N}_0$, has a macro element $K_T \in \mathcal{T}_0$ such that $T \subset K_T$. The generation $\text{gen}(T) \geq 0$ of an element $T \in \mathcal{T}_n$ is defined as*

$$\text{gen}(T) := \log_2 \left(\frac{|K_T|}{|T|} \right).$$

Definition 3.3 (Distance Function). *For two nodes $a, b \in \mathcal{N}(\mathcal{T})$, $a \neq b$, the distance function $\text{dist}(a, b) \in \mathbb{N}_0$ is defined as the minimal $J \in \mathbb{N}$ such that there exists elements T_1, \dots, T_J with*

$$a \in T_1, T_1 \cap T_2 \neq \emptyset, \dots, T_{J-1} \cap T_J \neq \emptyset, T_J \ni b.$$

For $a = b$, set $\text{dist}(a, a) = 0$. The distance to an element is defined as

$$\text{dist}(a, T) := \min \{ \text{dist}(a, b) : b \in \mathcal{N}(T) \}.$$

With this we can finally define

Definition 3.4 (Weight Function [16]). *For any $z \in \mathcal{V}(\mathcal{T})$ and a fixed parameter $\mu > 0$, define the weight*

$$h_z := \min \left\{ 2^{(\mu \text{dist}(z, T) - \text{gen}(T))/d} : T \in \mathcal{T} \right\}.$$

Then, for any $a \in \mathcal{N}(\mathcal{T}) \cap \mathcal{V}(\mathcal{T})$, h_a^+ is defined as above, while $h_a^- := (h_a)^{-1}$. For any $a \in \mathcal{N}(\mathcal{T}) \setminus \mathcal{V}(\mathcal{T})$, h_a^+ is defined⁵ by a linear interpolation of h_z^+ , $z \in \mathcal{V}(T) \cap \mathcal{N}(T)$. Analogously for h_a^- , $a \in \mathcal{N}(\mathcal{T}) \setminus \mathcal{V}(\mathcal{T})$.

Remark 3.5 (Correspondence to Other Criteria). *The framework introduced in Sections 2 and 3 covers the H^1 -stability criteria used in [4, 6, 7, 12, 16]. In particular, in [7] it was shown how the CT and BPS criteria correspond to a specific choice of weights h_z . The iterative approach introduced in [4] corresponds to $\mu = 2$ and, once again, a specific choice of h_z . Finally, in [16] the authors consider h_z as stated in Definition 3.4.*

To ensure that this choice of H_+ , H_- satisfies (C1) – (C3), we first check the conditions of Lemma 3.1, i.e., if $h_z \sim h_T$ for any $z \in \mathcal{V}(T)$ and any $T \in \mathcal{T}$. Note that one inequality is easily satisfied: for a sequence of admissible meshes $\{\mathcal{T}_n\}_{n=0}^\infty$, $z \in \mathcal{V}(T^*)$ and a macro element $K_{T^*} \supset T^*$, $K_{T^*} \in \mathcal{T}_0$, we have

$$\begin{aligned} h_z &= \min \left\{ 2^{(\mu \text{dist}(z, T) - \text{gen}(T))/d} : T \in \mathcal{T}_n \right\} \leq 2^{(\mu \text{dist}(z, T^*) - \text{gen}(T^*))/d} = 2^{-\text{gen}(T^*)/d} \\ &= (|T^*|/|K_{T^*}|)^{1/d} \lesssim h_{T^*} (1/|K_{T^*}|)^{1/d}, \end{aligned}$$

where we used the definition of $\text{gen}(\cdot)$ and the shape-regularity of \mathcal{T}_n . Thus, $h_z \lesssim h_T$ is easily satisfied with a constant depending only on \mathcal{T}_0 .

On the other hand, we have the critical inequality $h_T \lesssim h_z$. In principle this can always be satisfied by choosing $\mu > 0$ large enough. However, a larger $\mu > 0$ implies we allow for a larger rate of change for sizes of neighboring elements. We namely have

Lemma 3.6 ([7, 15, 16]). *For any $T \in \mathcal{T}$, it holds*

$$(3.3) \quad \max_{z, z' \in \mathcal{V}(T)} \frac{h_z}{h_{z'}} \leq 2^{\mu/d}.$$

The parameter $\mu > 0$ is determined by the refinement strategy and reflects the fact that neighboring elements $T, \bar{T} \in \mathcal{T}$ can vary in size upto

$$(3.4) \quad \max \{ |T|/|\bar{T}|, |\bar{T}|/|T| \} \lesssim 2^\mu.$$

We are thus interested in the smallest μ , for a given refinement strategy, satisfying (3.4), or, equivalently, satisfying $h_T \lesssim h_z$.

⁴This is the case for most common refinement strategies and also holds for the strategy considered in Section 4.1.

⁵This choice is slightly arbitrary and is made for convenience, as any choice satisfying (C1) – (C3) would be valid.

Remark 3.7 (Necessary Conditions). *The local conditions (C1) – (C3) from (3.2) are sufficient for H^1 -stability but are by no means necessary. The proof implicitly assumes that $h_T/h_{\bar{T}}$ increases exponentially with the distance between elements T and \bar{T} . Condition (C3) then ensures this exponential growth is counterbalanced by the exponential decay of $\|\Pi_h u_T\|_{0,\bar{T}}$, see also eq. (1.2), the discussion thereafter and Theorem 2.9. However, assuming consistent worst-case exponential growth for $h_T/h_{\bar{T}}$ is overly pessimistic and will not occur for many reasonable adaptively refined meshes \mathcal{T} , see also [4, Section 6].*

4. H^1 -STABILITY OF ADAPTIVELY REFINED QUADRILATERAL MESHES

As discussed in Section 3, to show H^1 -stability of a general mesh using weights as defined in Definition 3.4, we have to determine the smallest $\mu > 0$ for a given refinement strategy such that $h_T \lesssim h_z$, $z \in \mathcal{V}(T)$ and check whether the smallest eigenvalue in eq. (3.2) is positive. In this section, we proceed in two steps.

First, we vary $\mu = 1, 2, 3, 4$ and calculate for each μ and several reference elements the smallest eigenvalue in eq. (3.2). For a polynomial degree $p \in \mathbb{N}$, the corresponding conforming continuous Lagrange FE space \mathbb{V}_h is defined as the space of piece-wise polynomial functions such that (see also (2.1) and Definition 2.2)

- $(v_h)|_T \in \mathcal{P}_p(T)$ if T is a triangle,
- $(v_h)|_T \in \mathcal{Q}_p(T)$ if T is a quadrilateral,
- $v_h \in H^1(\Omega)$ and $v_h \notin H^2(\Omega)$.

We list these results in Appendix A.

Second, we use the results from Appendix A together with a proof for the minimal $\mu > 0$ to show H^1 -stability for the refinement strategy Q-RG from [3, 14] (see also Section 4.1). We will discuss the case of general quadrilaterals and non-linear transformations $B_T : \hat{T} \rightarrow T$ in Section 4.3, and conclude by showing H^1 -stability for Q-RB.

Remark 4.1 (Scope of Results). *The results in Appendix A are both used in this work to prove H^1 -stability for particular refinement strategies, and they are intended as a reference to check H^1 -stability for other refinement strategies not considered here. The corresponding code can be found in [1].*

Remark 4.2 (Calculating Eigenvalues in Equation (3.2)). *To calculate eigenvalues in eq. (3.2), we make use of a handy observation from [16]. For h_z as defined in Definition 3.4, for any $z \in \mathcal{V}(T^*)$, we have*

$$(4.1) \quad h_z^{-2} = \max \left\{ 2^{\text{gen}(T) - \mu \text{dist}(z,T)} : T \in \mathcal{T} \right\} \geq \text{gen}(T^*) \geq 0.$$

Moreover, the term $\text{gen}(T) - \mu \text{dist}(z,T)$ – due to the definition of $\text{dist}(z,T)$ and $\text{gen}(T)$ – can only attain values in a discrete set. E.g., for the refinement strategy Q-RG from [3, 14] (see also Section 4.1), $\text{gen}(T) \in \{0, 1, \log_2(8/3), 2, 3, 2 + \log_2(8/3), 4, 5, 4 + \log_2(8/3), \dots\}$. Thus, normalizing by the largest (or smallest) h_z in an element $T \in \mathcal{T}$, $z \in \mathcal{V}(T)$, together with eq. (4.1) and eq. (3.3), for any $T \in \mathcal{T}$ there is only a finite number of possible weight configurations. Consequently, in Appendix A we computed the smallest eigenvalue for each combination and took the minimum over all combinations.

4.1. Adaptive Refinement for Quadrilateral Meshes. In this subsection, we introduce some refinement strategies for quadrilateral meshes from [3, 14, 18, 24]. We consider three different strategies: red refinement Q-R, red-green refinement Q-RG and red-blue refinement Q-RB on quadrilaterals. Red, green and blue patterns used within these refinement strategies are depicted in Figure 1. Although these refinement strategies can be in principle applied to initial meshes of general quadrilaterals, we only consider initial meshes consisting of parallelograms in this work.

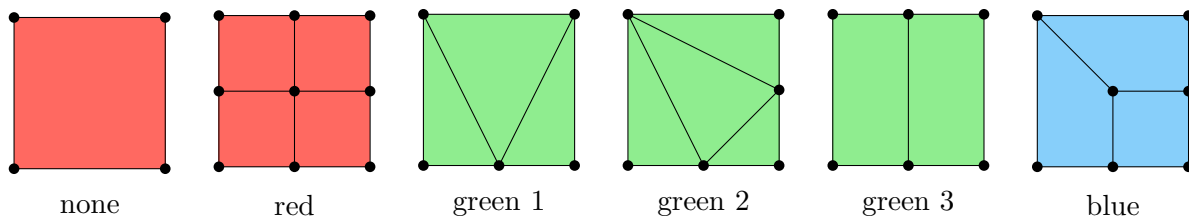


FIGURE 1. From left to right: Unrefined element, red pattern, three different green patterns and a blue pattern.

We call a quadrilateral *red*-refined if it is subdivided into four quadrilaterals by joining the midpoints of opposite edges with each other. We call a quadrilateral *green*-refined if it is divided into

- (1) three subtriangles by connecting the midpoint of one edge with the vertices opposite to this edge (green 1);
- (2) four subtriangles by joining the midpoints of two adjacent edges with the vertex shared by the other two edges with each other (green 2);
- (3) two subquadrilaterals by joining the midpoints of opposite edges with each other (green 3).

We call a quadrilateral *blue*-refined if it is divided into three subquadrilaterals by connecting the quadrilateral's midpoint with the two midpoints of adjacent edges and with the vertex shared by the other two edges with each other.

With this we can describe the refinement strategies Q-R in Algorithm 1, Q-RG in Algorithm 2 and Q-RB in Algorithm 3. Note, that for Q-R 1-irregularity of the mesh is ensured. We call a mesh \mathcal{T} *1-irregular* if the number of hanging nodes per edge is restricted to one. A node $z \in \mathcal{V}(\mathcal{T})$ is called a *hanging node* if for some element $T \in \mathcal{T}$ holds $z \in \partial T \setminus \mathcal{V}(\mathcal{T})$.

Algorithm 1 Q-R

- 1: **Input:** Mesh \mathcal{T} and set of marked elements \mathcal{T}_M .
 - 2: **Output:** Refined mesh $\hat{\mathcal{T}}$.
 - 3: **repeat**
 - 4: red-refine all $T \in \mathcal{T}_M$
 - 5: add elements with more than one hanging node per edge to \mathcal{T}_M ▷ 1-Irregularity
 - 6: add elements with more than three refined neighbors to \mathcal{T}_M ▷ 3-Neighbor Rule
 - 7: **until** $\mathcal{T}_M = \emptyset$
-

Remark 4.3 (Reference Elements for 1-Irregular Meshes). *For 1-irregular meshes, three different situations have to be considered: 0, 1 or 2 hanging nodes per element, see Figure 2. Other situations can not arise because a red refinement does not allow for any other combinations of hanging nodes.*

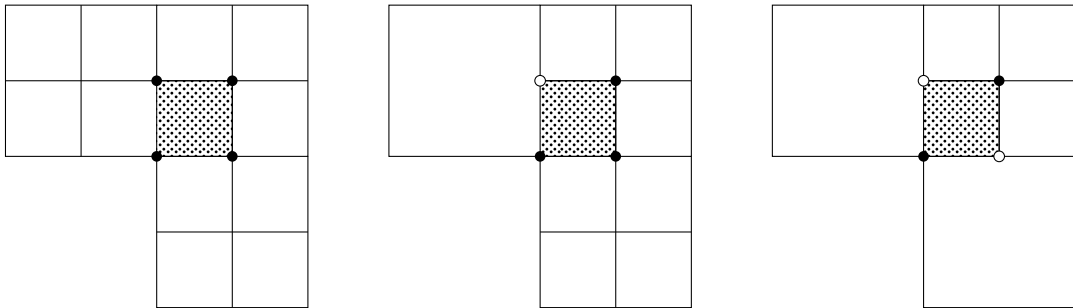


FIGURE 2. From left to right: 0, 1 and 2 hanging nodes (in white) per element (dotted).

Algorithm 2 Q-RG

- 1: **Input:** Mesh \mathcal{T} and set of marked elements \mathcal{T}_M .
 - 2: **Output:** Refined mesh $\hat{\mathcal{T}}$.
 - 3: Undo all green refinements and add their parent element to \mathcal{T}_M .
 - 4: Call Q-R with updated mesh and updated marked elements \mathcal{T}_M .
 - 5: Eliminate hanging nodes by matching green patterns.
-

Remark 4.4 (Generation of an Element). *Assume the initial mesh \mathcal{T}_0 consists of parallelograms. A red refinement quarters a parallelogram, i. e., the area ratios and thus the possible generations are given by*

$$\text{gen}(T) \in \{0, 2, 4, 6, \dots\},$$

for all $T \in \mathcal{T}$.

Algorithm 3 Q-RB

- 1: **Input:** Mesh \mathcal{T} and set of marked elements \mathcal{T}_M .
 - 2: **Output:** Refined mesh $\hat{\mathcal{T}}$.
 - 3: Undo all blue refinements and add their parent element to \mathcal{T}_M .
 - 4: Call Q-R with updated mesh and updated marked elements \mathcal{T}_M .
 - 5: Eliminate hanging nodes by matching blue patterns and an additional CLOSURE step, see [14].
-

For Q-RG we have

$$\text{gen}(T) \in \{0, 1, \log_2(8/3), 2, 3, 2 + \log_2(8/3), 4, 5, 4 + \log_2(8/3), \dots\},$$

for all $T \in \mathcal{T}$, cf. Figure 3. As green refinements are undone before they are further refined, the sequence continues in the same scheme.

As shown in Figure 1, not all elements of the blue patterns can be obtained by an affine transformation $B_T : \hat{T} \rightarrow T$ from $\hat{T} = [0, 1]^2$, see Section 4.3. We have for Q-RB that

$$\text{gen}(T) \in \{0, \log_2(8/3), 2, 2 + \log_2(8/3), 4, \dots\},$$

for all $T \in \mathcal{T}$.

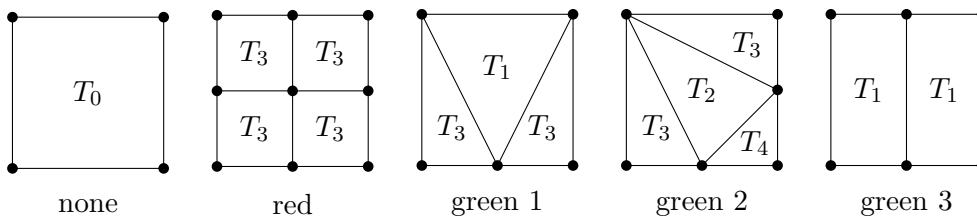


FIGURE 3. Area ratios for the refinement patterns in Q-RG: $|T_0|/|T_0| = 1$, $|T_0|/|T_1| = 2$, $|T_0|/|T_2| = 8/3$, $|T_0|/|T_3| = 4$ and $|T_0|/|T_4| = 8$.

4.2. Proof of H^1 -Stability. As was explained in Section 1.1 and Remark 3.7, H^1 -stability relies upon two competing effects: the localization properties of the L^2 -projection Π_h , which in turn depend on the polynomial degree of the FE space and the geometric shape of the elements; and the rate at which the mesh size is allowed to vary, which is reflected by the parameter μ .

It was already observed in [4, 16] for triangular meshes that the localization properties of Π_h improve at first for increasing polynomial degrees (up to $p = 5$ or $p = 6$), after which they start deteriorating again. This is also observed for quadrilateral meshes in Appendix A.

For increasing μ , the mesh size is allowed to vary more and this naturally leads to deteriorating constants as well.

Finally, in the presence of hanging nodes and due to the continuity constraint $\mathbb{V}_h \subset C(\Omega)$, the localization properties of Π_h deteriorate. A piece-wise polynomial continuous function with a non-zero value at one of the free nodes on the hanging edge (see Figure 2) has slightly larger support as it cannot be set to zero at the hanging node without violating the continuity constraint. This is reflected in Table 5 and Table 6 through deteriorating eigenvalues for 1 and 2 hanging nodes per element.

To show H^1 -stability we require the following lemma.

Lemma 4.5 (Minimal μ). *For the refinement strategies Q-R, Q-RG and Q-RB, an initial mesh \mathcal{T}_0 consisting of parallelograms and the choice $\mu = 2$ for the weights from Definition 3.4, we have $h_T \lesssim h_z$ for any $z \in \mathcal{V}(T)$, where the constant depends only on \mathcal{T}_0 .*

Proof. We closely follow the arguments in [8, 15]. We want to show that there are constants $\mu > 0$ and $C_\mu > 0$ only dependent on the initial mesh such that

$$(4.2) \quad \text{gen}(T') - \text{gen}(T) \leq \mu \text{dist}(z, z') + C_\mu \quad \forall T \in \mathcal{T}(z), T' \in \mathcal{T}(z'),$$

i.e., the difference in generations of two elements is bounded by a multiple of the distance and an additive constant, where $\mathcal{T}(z) := \{T \in \mathcal{T} \mid z \in T\}$. Then, eq. (4.2) would readily imply $h_T \lesssim h_z$ for

any $z \in \mathcal{V}(T)$. This can be seen as follows. For any $T \in \mathcal{T}$, there is a macro element $K_T \in \mathcal{T}_0$ such that $T \subset K_T$. For $z \in \mathcal{V}(T)$ let T' and $z' \in T'$ be such that the weight h_z satisfies

$$h_z^2 = 2^{\mu \operatorname{dist}(z, T') - \operatorname{gen}(T')} = 2^{\mu \operatorname{dist}(z, z') - \operatorname{gen}(T')}.$$

Using eq. (4.2) and recalling the definition of $\operatorname{gen}(\cdot)$, we conclude

$$h_z^2 \geq 2^{-C_\mu - \operatorname{gen}(T)} = 2^{-C_\mu} \frac{|T|}{|K_T|} \geq Ch_T^2$$

with $C := 2^{-C_\mu} \frac{1}{|K_T|}$ only dependent on the initial mesh. This shows $h_T \lesssim h_z$ for any $z \in \mathcal{V}(T)$.

It thus remains to show eq. (4.2) with $\mu = 2$ and a suitable choice of C_μ . Fix some $z, z' \in \mathcal{V}(\mathcal{T})$ and consider the shortest path of elements connecting z and z' , i.e.,

$$\operatorname{PE}(z, z') := \{z = z_0, z_1, \dots, z_{M-1}, z_M = z'\},$$

where z_{i-1} and z_i belong to the same element, $i = 1, \dots, M$, and M is minimal. We proceed in three steps.

(1) For any $z \in \mathcal{V}(T)$ we bound

$$\operatorname{gen}(T) - \operatorname{gen}(T') \leq \begin{cases} \alpha, & z \in \mathcal{V}(\mathcal{T}) \setminus \mathcal{V}(\mathcal{T}_0) \\ \alpha_0, & z \in \mathcal{V}(\mathcal{T}_0) \end{cases} \quad \text{for all } T, T' \in \mathcal{T}(z).$$

Let $z \in \mathcal{V}(\mathcal{T}_0)$. An upper bound is given by $\alpha_0 = \max \{\#\mathcal{T}_0(z_0) \mid z_0 \in \mathcal{V}(\mathcal{T}_0)\}$ for Q-R, Q-RG and Q-RB. The generation increases at most by 2 when crossing an edge of a macro element and we can traverse from the element with minimal generation to maximal generation by crossing at most $\lfloor \#\mathcal{T}_0(z_0)/2 \rfloor$ macro elements.

Let $z \in \mathcal{V}(\mathcal{T}) \setminus \mathcal{V}(\mathcal{T}_0)$. The possible maximal differences of generations are shown in Figure 4 and yield $\alpha = 2$ for Q-RB, $\alpha = 3$ for Q-RG and $\alpha = 4$ for Q-R.

(2) For any $z, z' \in \mathcal{V}(\mathcal{T}) \setminus \mathcal{V}(\mathcal{T}_0)$, we consider the maximal difference of generations for all elements $T \in \mathcal{T}(z)$, $T' \in \mathcal{T}(z')$, where $\operatorname{PE}(z, z') \cap \mathcal{V}(\mathcal{T}_0) = \emptyset$. By the above considerations, a straight-forward upper bound would be

$$\operatorname{gen}(T) - \operatorname{gen}(T') \leq \alpha \#\operatorname{PE}(z, z') \quad \text{for all } T \in \mathcal{T}(z), T' \in \mathcal{T}(z').$$

Figure 4 shows meshes yielding the maximal difference of generation. For Q-RB this bound can not be improved because a sequence of scaled versions can be inserted into the most upper left quadrilateral, showing that this bound is optimal.

For Q-RG we can improve this bound. To this end, for $i = 1, \dots, M$, set

$$T_i = \arg \max \{\operatorname{gen}(T) \mid T \in \mathcal{T}, z_{i-1}, z_i \in T\}.$$

Without loss of generality, we only consider generation increases. We see that the generation difference 3 can only be attained once in a path – namely $\operatorname{gen}(T_1) = \operatorname{gen}(T) + 3$ for some $T \in \mathcal{T}(z)$ – and otherwise $\operatorname{gen}(T_i) = \operatorname{gen}(T_{i-1}) + 2$ for $i = 2, \dots, M$. We can thus conclude the upper bound

$$\operatorname{gen}(T) - \operatorname{gen}(T') \leq 2\#\operatorname{PE}(z, z') + 1 \quad \text{for all } T \in \mathcal{T}(z), T' \in \mathcal{T}(z').$$

Note, that other situations than the one shown in Figure 4 can arise that also satisfy this reduced upper bound.

For Q-R, improving the upper bound is a bit more involved, cf. [15, Proposition 3.8]. Two reference situations for Q-R are shown in Figure 4. These show that in between two generation differences of 4, there must be one generation difference of 0, with any possible number of generation differences of 2 in between. Let N_4 denote the number of indices with generation difference 4 within $\operatorname{PE}(z, z')$. Using a telescopic sum this yields

$$\begin{aligned} \operatorname{gen}(T) - \operatorname{gen}(T') &= \sum_{i=0}^M \operatorname{gen}(T_{i+1}) - \operatorname{gen}(T_i) \\ &\leq 2\#\operatorname{PE}(z, z') + 2N_4 - 2(N_4 - 1) = 2\#\operatorname{PE}(z, z') + 2. \end{aligned}$$

Thus, for all strategies, we have a common upper bound $2\#\operatorname{PE}(z, z') + 2$.

(3) We now take a minimal path connecting z and z' and split the path into pieces $\operatorname{PE}(z, z') \setminus \mathcal{V}(\mathcal{T}_0)$ and $z \in \mathcal{V}(\mathcal{T}_0)$, i.e.,

$$\operatorname{PE}(z, z') = \operatorname{PE}(z, z_1) \cup \{z_1\} \cup \operatorname{PE}(z_1, z_2) \cup \dots \cup \{z_J\} \cup \operatorname{PE}(z_J, z'),$$

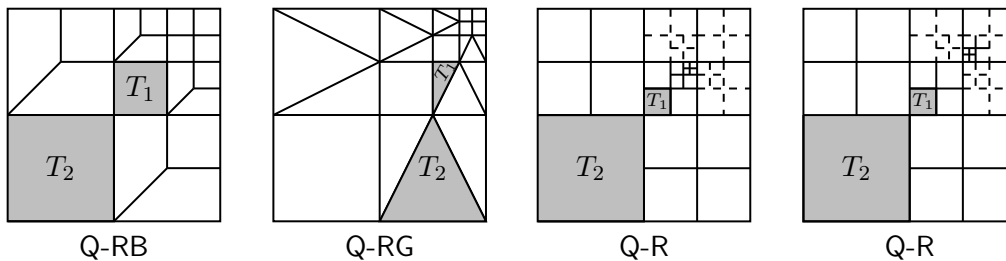


FIGURE 4. Maximal differences of generations. $\text{gen}(T_2) - \text{gen}(T_1) = 2$ for Q-RB, 3 for Q-RG and 4 for Q-R.

where J vertices from the initial mesh are contained in $\text{PE}(z, z')$. We can thus conclude that the bound for all $z, z' \in \mathcal{V}(\mathcal{T})$ is

$$\begin{aligned} \text{gen}(T) - \text{gen}(T') &\leq \sum_{j=0}^J (2\#\text{PE}(z_j, z_{j+1}) + 2) + \sum_{j=1}^J \alpha_0 \\ &\leq 2\#\text{PE}(z, z') + 2(J + 1) + J\alpha_0 \end{aligned}$$

for all $T \in \mathcal{T}(z), T' \in \mathcal{T}(z')$. Minimality of $\text{PE}(z, z')$ gives $\text{PE}(z, z') = \text{dist}(z, z') + 1$ and $J \leq \#\mathcal{V}(\mathcal{T}_0)$. This shows eq. (4.2) with $\mu = 2$ and $C_\mu = 4 + \#\mathcal{V}(\mathcal{T}_0)(\alpha_0 + 1)$. \square

With this we can show

Theorem 4.6 (H^1 -Stability for Q-RG). *For any initial mesh \mathcal{T}_0 consisting of parallelograms, Q-RG is H^1 -stable for polynomial degrees $p = 2, \dots, 9$.*

Remark 4.7 (Hanging Nodes). *The refinement strategy Q-R satisfies $h_T \lesssim h_z$ for $\mu = 2$. However, due to hanging nodes, the localization properties of Π_h are too unfavorable such that H^1 -stability can only be guaranteed for the restricted case $\mu = 1$ and $p = 1, 2$.*

4.3. General Quadrilaterals and Non-Linear Transformations. In Theorem 4.6 and Remark 4.7 we addressed meshes where each element T can be obtained by an affine transformation $B_T : \hat{T} \rightarrow T$ onto $\hat{T} = [0, 1]^2$ or $\hat{T} = \{(\hat{x}, \hat{y})^\top \in [0, 1]^2 : 0 \leq \hat{x} + \hat{y} \leq 1\}$. However, if we use the refinement strategy Q-RB from [14] (see also Section 4.1) with an initial mesh consisting of parallelograms – such elements can only be obtained through a non-linear transformation $B_T : \hat{T} \rightarrow T$. The theory introduced above remains unchanged for this case. However, the computation of the eigenvalue problem in eq. (3.2) is now more involved since it cannot be performed entirely independent of T .

For a general quadrilateral $T \in \mathcal{T}$, we introduce the bilinear transformation $B_T : [0, 1]^2 \rightarrow T$

$$(4.3) \quad B_T \begin{pmatrix} \hat{x} \\ \hat{y} \end{pmatrix} := \begin{pmatrix} x_0 \\ y_0 \end{pmatrix} + \begin{pmatrix} \cos(\theta) & -\sin(\theta) \\ \sin(\theta) & \cos(\theta) \end{pmatrix} \left[\begin{pmatrix} 1 & s \\ 0 & 1 \end{pmatrix} \begin{pmatrix} h_x & 0 \\ 0 & h_y \end{pmatrix} \begin{pmatrix} \hat{x} \\ \hat{y} \end{pmatrix} + \begin{pmatrix} \alpha \hat{x} \hat{y} \\ \beta \hat{x} \hat{y} \end{pmatrix} \right],$$

where we used a convenient representation from [5]. The free parameters $x_0, y_0, \theta, s, h_x, h_y, \alpha$ and β depend on T . Any general quadrilateral in 2D can be obtained by using this transformation.

The parameters $(x_0, y_0)^\top \in \mathbb{R}^2$ describe translation of the reference point $(0, 0)^\top$. The parameter $\theta \in [0, 2\pi)$ describes rotation. The parameters $h_x, h_y > 0$ describe stretching of the horizontal side $(1, 0)^\top$ and the vertical side $(0, 1)^\top$, respectively.

The parameter s describes shearing of the square $[0, 1]^2$. I.e., for $s = 0$ (and $\alpha = \beta = 0$), T is a rectangle with side lengths h_x and h_y . The larger s , the larger the stretching of the rectangle to a parallelogram. To maintain shape-regularity, the shearing s has to remain bounded in absolute value.

Finally, $\alpha, \beta \in \mathbb{R}$ control the non-linear part of the transformation. I.e., for $\alpha = \beta = 0$, T is a parallelogram. Loosely speaking, for $\alpha > 0$, T becomes a trapezoid due to shifting of the reference point $(1, 1)^\top$ horizontally, and similarly for $\beta > 0$ vertically.

Computing the determinant of the Jacobian we obtain

$$\left| \det DB_T \begin{pmatrix} \hat{x} \\ \hat{y} \end{pmatrix} \right| = h_x h_y + h_x \beta \hat{x} + h_y (\alpha - \beta s) \hat{y}.$$

For $\alpha = \beta = 0$, i. e., the affine case, this reduces to $\left| \det DB_T \begin{pmatrix} \hat{x} \\ \hat{y} \end{pmatrix} \right| = h_x h_y = |T|$. The new element mass matrix (without hanging nodes) is

$$M(T) = h_x h_y M_L + h_x \beta M_x + h_y (\alpha - \beta s) M_y \in \mathbb{R}^{\#\mathcal{N}(T) \times \#\mathcal{N}(T)},$$

with

$$\begin{aligned} (M_L)_{a,b} &:= \int_{[0,1]^2} \hat{\varphi}_a(\hat{x}, \hat{y}) \hat{\varphi}_b(\hat{x}, \hat{y}) \, d\hat{x} \, d\hat{y}, \\ (M_x)_{a,b} &:= \int_{[0,1]^2} \hat{\varphi}_a(\hat{x}, \hat{y}) \hat{\varphi}_b(\hat{x}, \hat{y}) \hat{x} \, d\hat{x} \, d\hat{y}, \\ (M_y)_{a,b} &:= \int_{[0,1]^2} \hat{\varphi}_a(\hat{x}, \hat{y}) \hat{\varphi}_b(\hat{x}, \hat{y}) \hat{y} \, d\hat{x} \, d\hat{y}, \end{aligned}$$

for $a, b \in \mathcal{N}(\hat{T})$. The matrix $A(T)$ from eq. (3.2) is adjusted accordingly to

$$A(T) = h_x h_y A_L + h_x \beta A_x + h_y (\alpha - \beta s) A_y.$$

Dividing both sides of eq. (3.2) by $h_x h_y$, we obtain the generalized eigenvalue problem

$$\left(A_L + \frac{\beta}{h_y} A_x + \frac{\alpha - \beta s}{h_x} A_y \right) x =: \hat{A}x = \lambda \hat{M}x := \lambda \left(M_L + \frac{\beta}{h_y} M_x + \frac{\alpha - \beta s}{h_x} M_y \right) x, \quad x \in \mathbb{R}^{\#\mathcal{N}(\hat{T})}.$$

We can now compute the smallest eigenvalue of the above problem under some reasonable assumptions on the degree of non-linearity. E. g., for some constant $0 < c < 1$, assume the non-linearity of T is bounded as

$$(4.4) \quad |\alpha| \leq c h_x, \quad |\beta| \leq c \min \left\{ h_y, \frac{h_x}{s} \right\}.$$

These assumptions were used in, e. g., [5] (with $c = 1/4$) to show H^1 -stability of a Scott-Zhang type projector onto general anisotropic quadrilateral meshes. With this we obtain the bounds

$$\frac{|\beta|}{h_y} \leq c, \quad \frac{|\alpha - \beta s|}{h_x} \leq 2c.$$

Thus, for any given adaptive refinement strategy in 2D with general quadrilaterals, H^1 -stability follows from (4.4), Table 3 and the following lemma.

Lemma 4.8 (H^1 -Stability General Quadrilaterals). *Consider the generalized eigenvalue problem*

$$(4.5) \quad \hat{A}x = \lambda \hat{M}x, \quad x \in \mathbb{R}^n, \quad n \in \mathbb{N},$$

with

$$\hat{A} := A_L + c_1 A_x + c_2 A_y, \quad \hat{M} := M_L + c_1 M_x + c_2 M_y, \quad (c_1, c_2)^\top \in [-c, c] \times [-2c, 2c], \quad c > 0,$$

satisfying

- (i) \hat{M} is symmetric positive definite for any $(c_1, c_2)^\top \in [-c, c] \times [-2c, 2c]$,
- (ii) A_L, A_x and A_y are symmetric.

Let $\lambda_{\min}(c_1, c_2)$ denote the smallest eigenvalue of eq. (4.5). If the smallest eigenvalue satisfies

$$\inf_{\substack{-c \leq c_1 \leq c, \\ -2c \leq c_2 \leq 2c}} \lambda_{\min}(c_1, c_2) \leq 0,$$

then we have $\lambda_{\min}(c_1, c_2) \leq 0$ for some

$$(c_1, c_2)^\top \in \left\{ \begin{pmatrix} -c \\ -2c \end{pmatrix}, \begin{pmatrix} c \\ -2c \end{pmatrix}, \begin{pmatrix} -c \\ 2c \end{pmatrix}, \begin{pmatrix} c \\ 2c \end{pmatrix}, \begin{pmatrix} 0 \\ 0 \end{pmatrix} \right\}.$$

In other words, to ensure all eigenvalues are strictly positive we only have to check 5 combinations $(c_1, c_2)^\top$.

Proof. The smallest eigenvalue of eq. (4.5) is characterized by minimizing the Rayleigh quotient

$$\lambda_{\min}(c_1, c_2) = \min_{x \in \mathbb{R}^n \setminus \{0\}} R_{c_1, c_2}(x) := \frac{\langle x, \hat{A}x \rangle}{\langle x, \hat{M}x \rangle}.$$

The denominator is always positive since we assumed $\hat{M} > 0$, i. e., \hat{M} is symmetric positive definite. Thus, $\lambda_{\min}(c_1, c_2) \leq 0$ can only occur if $\langle x, \hat{A}x \rangle \leq 0$. For the latter we have

$$(4.6) \quad \langle x, \hat{A}x \rangle = \langle x, A_L x \rangle + c_1 \langle x, A_x x \rangle + c_2 \langle x, A_y x \rangle.$$

Each of the matrices A_L , A_x and A_y have real eigenvalues that can be either positive or negative. The statement of the lemma simply follows by considering the $2^3 = 8$ possibilities.

E.g., if $A_L \leq 0$, then we can obtain $\lambda_{\min}(c_1, c_2) \leq 0$ for $c_1 = c_2 = 0$. If $A_L > 0$ and $A_x > 0$, $A_y \leq 0$, then, if the sum in Equation (4.6) is negative or zero for some $x \in \mathbb{R}^n \setminus \{0\}$, it will certainly hold for $c_1 = -c$ and $c_2 = 2c$. Analogously for all other cases. \square

The quadrilaterals of a blue pattern can be obtained by the bilinear transformation B_T from (4.3) with $c_2 \in \{-1/2, 0, 1\}$ and $c_1 = 0$. It thus follows from Table 4 and Lemma 4.5

Theorem 4.9 (H^1 -Stability for Q-RB). *For any initial mesh \mathcal{T}_0 consisting of parallelograms, Q-RB is H^1 -stable for polynomial degrees $p = 2, \dots, 9$.*

REFERENCES

- [1] ALI, M., FUNKEN, S. A., AND SCHMIDT, A. Codes on the H^1 -Stability of the L^2 -Projection. Code download at <https://github.com/aschmidtuulm/h1-stability>, 2020.
- [2] AURADA, M., FEISCHL, M., KEMETMÜLLER, J., PAGE, M., AND PRAETORIUS, D. Each $H^{1/2}$ -Stable Projection yields Convergence and Quasi-Optimality of Adaptive FEM with Inhomogeneous Dirichlet Data in R^d . *ESAIM: M2AN* 47, 4 (2013), 1207–1235.
- [3] BANK, R. E., SHERMAN, A. H., AND WEISER, A. Some Refinement Algorithms and Data Structures for Regular Local Mesh Refinement. *Scientific Computing, Applications of Mathematics and Computing to the Physical Sciences 1* (1983), 3–17.
- [4] BANK, R. E., AND YSERENTANT, H. On the H^1 -Stability of the L_2 -Projection onto Finite Element Spaces. *Numerische Mathematik* 126 (2014), 361–381.
- [5] BRAACK, M. Anisotropic H^1 -Stable Projections on Quadrilateral Meshes. In *Numerical Mathematics and Advanced Applications* (Berlin, Heidelberg, 2006), A. B. de Castro, D. Gómez, P. Quintela, and P. Salgado, Eds., Springer Berlin Heidelberg, pp. 495–503.
- [6] BRAMBLE, J. H., PASCIAK, J. E., AND STEINBACH, O. On the Stability of the L^2 Projection in $H^1(\Omega)$. *Mathematics of Computation* 71, 237 (2002), 147–156.
- [7] CARSTENSEN, C. Merging the Bramble-Pasciak-Steinbach and the Crouzeix-Thomee Criterion for H^1 -Stability of the L^2 -Projection onto Finite Element Spaces. *Mathematics of Computation* 71, 237 (2002), 157–163.
- [8] CARSTENSEN, C. An Adaptive Mesh-Refining Algorithm Allowing for an H^1 -Stable L^2 -Projection onto Courant Finite Element Spaces. *Constructive Approximation* 20, 4 (oct 2003), 549–564.
- [9] CARSTENSEN, C., AND HU, J. Hanging Nodes in the Unifying Theory of a Posteriori Finite Element Error Control. *Journal of Computational Mathematics* 27, 2/3 (2009), 215–236.
- [10] CARSTENSEN, C., AND VERFÜRTH, R. Edge Residuals Dominate A Posteriori Error Estimates for Low Order Finite Element Methods. *SIAM Journal on Numerical Analysis* 36, 5 (1999), 1571–1587.
- [11] CLÉMENT, P. Approximation by Finite Element Functions using Local Regularization. *ESAIM: Mathematical Modelling and Numerical Analysis - Modélisation Mathématique et Analyse Numérique* 9, R2 (1975), 77–84.
- [12] CROUZEIX, M., AND THOMÉE, V. The Stability in L_p and W_p^1 of the L_2 -Projection onto Finite Element Function Spaces. *Mathematics of Computation* 48, 178 (1987), 521–532.
- [13] DEMKO, S., MOSS, W. F., AND SMITH, P. W. Decay Rates for Inverses of Band Matrices. *Mathematics of Computation* 43, 168 (1984), 491–499.
- [14] FUNKEN, S. A., AND SCHMIDT, A. Adaptive Mesh Refinement in 2D – An Efficient Implementation in Matlab. *Computational Methods in Applied Mathematics* 20, 3 (jul 2020), 459–479.
- [15] GASPOZ, F. D., HEINE, C.-J., AND SIEBERT, K. G. Optimal Grading of the Newest Vertex Bisection and H^1 -Stability of the L_2 -Projection. *IMA Journal of Numerical Analysis* 36, 3 (10 2015), 1217–1241.
- [16] GASPOZ, F. D., HEINE, C.-J., AND SIEBERT, K. G. An Alternative Proof of the H^1 -Stability of the L_2 -Projection on Graded Meshes. Tech. rep., Fachbereich Mathematik, Universität Stuttgart, 2019.
- [17] KARKULIK, M., PAVLICEK, D., AND PRAETORIUS, D. On 2D Newest Vertex Bisection: Optimality of Mesh-Closure and H^1 -Stability of L_2 -Projection. *Constructive Approximation* 38, 2 (may 2013), 213–234.
- [18] KOBBELT, L. Interpolatory Subdivision on Open Quadrilateral Nets with Arbitrary Topology. *Computer Graphics Forum* 15, 3 (1996), 409–420.
- [19] MCLEAN, W., AND STEINBACH, O. Boundary Element Preconditioners for a Hypersingular Integral Equation on an Interval. *Advances in Computational Mathematics* 11, 4 (1999), 271–286.
- [20] SCOTT, L. R., AND ZHANG, S. Finite Element Interpolation of Nonsmooth Functions Satisfying Boundary Conditions. *Mathematics of Computation* 54, 190 (1990), 483–493.
- [21] STEINBACH, O. On a Hybrid Boundary Element Method. *Numerische Mathematik* 84, 4 (feb 2000), 679–695.
- [22] STEINBACH, O., AND WENDLAND, W. The Construction of some Efficient Preconditioners in the Boundary Element Method. *Advances in Computational Mathematics* 9, 1/2 (1998), 191–216.

- [23] TANTARDINI, F., AND VEESER, A. The L^2 -Projection and Quasi-Optimality of Galerkin Methods for Parabolic Equations. *SIAM Journal on Numerical Analysis* 54, 1 (2016), 317–340.
- [24] VERFÜRTH, R. *A review of a posteriori error estimation and adaptive mesh-refinement techniques*. John Wiley & Sons Inc, 1996.
- [25] WAHLBIN, L. B. *Superconvergence in Galerkin Finite Element Methods*. Springer Berlin Heidelberg, 1995.
- [26] YSERENTANT, H. Old and New Convergence Proofs for Multigrid Methods. *Acta Numerica* 2 (1993), 285–326.

APPENDIX A. TABLES

TABLE 1. Triangular element with no hanging nodes.

$\mu = 1$		$\mu = 2$	
p	λ_{\min}	p	λ_{\min}
1	0.917136664350836	1	0.658493649053890
2	0.951669246453928	2	0.800813482191006
3	0.964185270379702	3	0.852396026216779
4	0.968240261180467	4	0.869107942296914
5	0.966806486169801	5	0.863198896177376
6	0.959408791893528	6	0.832710628261139
7	0.943501297553834	7	0.767150748223897
8	0.913475197477444	8	0.643403571141314
9	0.859176805106264	9	0.419622502039389
10	0.762190410650697	10	0.019910501521261
11	0.589258437047241	11	-0.692797559342644
12	0.279511860034300	12	-1.969362428534202

$\mu = 3$		$\mu = 4$	
p	λ_{\min}	p	λ_{\min}
1	0.192692294634035	1	-0.536778579257494
2	0.529130834062903	2	0.103660669859525
3	0.651069958003112	3	0.335782117975507
4	0.690576276364528	4	0.410985740336119
5	0.676607521609456	5	0.384395032798194
6	0.604534444362571	6	0.247197827175128
7	0.449553442778550	7	-0.047821632992457
8	0.157019938498792	8	-0.604683929864082
9	-0.371989788261829	9	-1.611698740822758
10	-1.316893380981366	10	-3.410402743154268
11	-3.001707463114409	11	-6.617589017041926
12	-6.019457067017003	12	-12.362130928403941

TABLE 2. Parallelogram element with no hanging nodes. Note that for $\mu = 2$ and $p = 1$, λ_{\min} is *exactly* 0, i.e., this represents a “border” case.

$\mu = 1$		$\mu = 2$	
p	λ_{\min}	p	λ_{\min}
1	0.757359312880714	1	0.000000000000000
2	0.909009742330268	2	0.625000000000000
3	0.944316491021463	3	0.770510421645976
4	0.956248179064318	4	0.819684730309997
5	0.958418441371873	5	0.828629076508982
6	0.952907970706445	6	0.805918661652962
7	0.935573718078176	7	0.734478653655678
8	0.890974043187541	8	0.550669106212760
9	0.773040724644832	9	0.064628121319203
10	0.445576028516330	10	-1.284958792632702

$\mu = 3$		$\mu = 4$	
p	λ_{\min}	p	λ_{\min}
1	-1.363961030678928	1	-3.500000000000000
2	0.113514613495402	2	-0.687500000000000
3	0.457495579824147	3	-0.032703102593110
4	0.573741729216471	4	0.188581286394985
5	0.594885815075774	5	0.228830844290421
6	0.541199279365591	6	0.126633977438330
7	0.372317884428622	7	-0.194846058549442
8	-0.062200722793164	8	-1.021989022042573
9	-1.211182670394353	9	-3.209173454063614
10	-4.401553542490907	10	-9.282314566847294

TABLE 3. General quadrilateral element with no hanging nodes and $c = 1/4$, see eq. (4.4).

$\mu = 1$		$\mu = 2$	
p	λ_{\min}	p	λ_{\min}
1	0.747149409107802	1	-0.042078284125092
2	0.905648684583979	2	0.611148004334341
3	0.942338691490434	3	0.762359276203259
4	0.954647079121367	4	0.813086084543036
5	0.956761324592774	5	0.821799567415631
6	0.950779093984766	6	0.797144878710977
7	0.932233847358632	7	0.720713976514372
8	0.884721376019483	8	0.524899861811526
9	0.759489811676522	9	0.008780468029065
10	0.412406997710229	10	-1.421658994070072

$\mu = 3$		$\mu = 4$	
p	λ_{\min}	p	λ_{\min}
1	-1.463432454588482	1	-3.689352278562916
2	0.080769035544651	2	-0.749833980495465
3	0.438226589642168	3	-0.069383257085339
4	0.558142787768123	4	0.158887380443665
5	0.578741121720422	5	0.198098053370336
6	0.520458398399101	6	0.087151954199392
7	0.339778724066694	7	-0.256787105685328
8	-0.123118212347723	8	-1.137950621848126
9	-1.343204346427102	9	-3.460487893869209
10	-4.724707491574776	10	-9.897465473315364

TABLE 4. General quadrilateral element with no hanging nodes, $c_1 = 0$ and $c_2 \in \{-1/2, 0, 1\}$, see eq. (4.5).

$\mu = 1$		$\mu = 2$	
p	λ_{\min}	p	λ_{\min}
1	0.752122198173689	1	-0.021583827383621
2	0.907368513818204	2	0.618235971544799
3	0.943368537006528	3	0.766603599479458
4	0.955486626928499	4	0.816546129999960
5	0.957630538869594	5	0.825381877897596
6	0.951888510846911	6	0.801717140994429
7	0.933947667570817	7	0.727777178620049
8	0.887854856425997	8	0.537813938357047
9	0.766127960891231	9	0.036138407431271
10	0.428435362614456	10	-1.355600967716399

$\mu = 3$		$\mu = 4$	
p	λ_{\min}	p	λ_{\min}
1	-1.414984357506708	1	-3.597127223226294
2	0.097524713816906	2	-0.717938128048401
3	0.448260004468708	3	-0.050283802342439
4	0.566322200392669	4	0.174457584999823
5	0.587209564099582	5	0.214218450539184
6	0.531267048259225	6	0.107727134474930
7	0.356475858596323	7	-0.225002696209782
8	-0.092589838646902	8	-1.079837277393274
9	-1.278531243800609	9	-3.337377166559288
10	-4.568548891511071	10	-9.600204354723619

TABLE 5. Parallelogram element with 1 hanging node.

$\mu = 1$		$\mu = 2$	
p	λ_{\min}	p	λ_{\min}
1	0.5713583436501	1	-0.7665695784117
2	0.5111112137989	2	-1.0321608739122
3	-0.4908310649897	3	-5.1703397243886
4	-5.0403752099103	4	-23.9128701137892
5	-28.0738045059095	5	-118.8224619748803

$\mu = 3$		$\mu = 4$	
p	λ_{\min}	p	λ_{\min}
1	-3.1761016413483	1	-6.9495631028529
2	-3.8842461768688	2	-8.5676118293778
3	-13.7037380407129	3	-27.3679339412646
4	-57.9779496110135	4	-111.5515607551863
5	-282.2556307086560	5	-538.2010788870381

TABLE 6. Parallelogram element with 2 hanging nodes.

$\mu = 1$		$\mu = 2$	
p	λ_{\min}	p	λ_{\min}
1	0.3509421918476	1	-1.6749751488843
2	0.1968076252802	2	-2.3102130737245
3	-1.3306311581102	3	-8.6052776052544
4	-8.3677990882113	4	-37.6077009566311
5	-42.9093635066812	5	-179.9645530924988

$\mu = 3$		$\mu = 4$	
p	λ_{\min}	p	λ_{\min}
1	-5.3235370099972	1	-11.0373881699796
2	-6.8252147095288	2	-13.8959588317600
3	-21.7065019476733	3	-42.2237492236424
4	-90.2671005455771	4	-172.7346543048027
5	-426.7931514447289	5	-813.3404889159924